

Research Article

Aleksandar Valjarević*, Marija Milić, Dragana Valjarević, Zorica Stanojević-Ristić, Ljiljana Petrović, Miško Milanović, Dejan Filipović, Branko Ristanović, Biljana Basarin, and Tin Lukić

Modelling and mapping of the COVID-19 trajectory and pandemic paths at global scale: A geographer's perspective

<https://doi.org/10.1515/geo-2020-0156>

received May 23, 2020; accepted November 05, 2020

Abstract: In December 2019, the virus SARS-CoV-2 responsible for the COVID-19 pandemic was detected in the Chinese city of Wuhan. The virus started to spread from China and dispersed over the rest of the world. In March 2020, WHO (World Health Organization) declared COVID-19 a pandemic. The transmission path of the pandemic was accelerated by different types of transportation. With complete analysis of spatial data, population

density, types of traffic networks, and their properties, the spatial distribution of COVID-19 was estimated. GIS (Geographical Information System), numerical methods, and software for network analysis were used in this research to model scenarios of virus distribution on a global scale. The analyzed data included air, railway, marine, and road traffic. In the pandemic research, numerous models of possible trajectory of viruses can be created. Many have a stochastic character. This study includes all countries in the world affected by the COVID-19 up to date. In this study, GIS methods such as buffer, interpolations, and numerical analysis were used in order to estimate and visualize ongoing COVID-19 pandemic situation. According to the availability of new data, trajectory of virus paths was estimated. On the other hand, sparsely populated areas with poorly developed and small traffic networks (and isolated island territories) tend to be less or not affected as shown by the model. This low-cost approach can be used in order to define important measures that need to be addressed and implemented in order to successfully mitigate the implications of COVID-19 not only on global, but local and regional scales as well.

Keywords: COVID-19, GIS, progressions, traffic types, modelling, mapping

* **Corresponding author: Aleksandar Valjarević**, Department for Management of Science and Technology Development, Ton Duc Thang University, Ho Chi Minh City, Viet Nam
Faculty of Environment and Labour Safety, Ton Duc Thang University, Ho Chi Minh City, Viet Nam,
e-mail: aleksandar.valjarevic@tdtu.edu.vn

Marija Milić: Department of Epidemiology, Faculty of Medicine, University of Priština - Kosovska Mitrovica, Kosovska Mitrovica, Serbia, e-mail: marijamilic85@gmail.com

Dragana Valjarević: Department of Mathematics, Faculty of Sciences, University in Priština - Kosovska Mitrovica, Kosovska Mitrovica, Serbia, e-mail: dragana.valjarevic@pr.ac.rs

Zorica Stanojević-Ristić: Institute of Pharmacology and Toxicology, Faculty of Medicine, University of Priština - Kosovska Mitrovica, Kosovska Mitrovica, Serbia, e-mail: zorica.stanojevic@med.pr.ac.rs

Ljiljana Petrović: Department of Mathematics and Statistics, Faculty of Economics, University of Belgrade, Belgrade, Serbia,
e-mail: petrovl@ekof.bg.ac.rs

Miško Milanović: University of Belgrade, Faculty of Geography, Department of Geospatial and Environmental Science, Studentski Trg 3/III, Belgrade, Serbia, e-mail: milanovic.misko@gmail.com

Dejan Filipović: University of Belgrade, Faculty of Geography, Department of Spatial Planning, Studentski Trg 3/III, Belgrade, Serbia, e-mail: prof.dejanf@gmail.com

Branko Ristanović: University of Novi Sad, Faculty of Sciences, Department of Geography, Tourism and Hotel Management, Trg Dositeja Obradovića 3, 21000 Novi Sad, Serbia,
e-mail: brankoris@yahoo.com

Biljana Basarin: University of Novi Sad, Faculty of Sciences, Department of Geography, Tourism and Hotel Management, Trg Dositeja Obradovića 3, 21000 Novi Sad, Serbia,
e-mail: biljana.basarin@gmail.com

Tin Lukić: University of Novi Sad, Faculty of Sciences, Department of Geography, Tourism and Hotel Management, Trg Dositeja Obradovića 3, 21000 Novi Sad, Serbia, e-mail: lukic021@gmail.com

1 Introduction

Modern society has forgotten the danger of infectious diseases, and relying on medical advancement created a zone of false comfort, by suppressing the memory of many outbreaks and pandemics that have occurred throughout history [1,2]. The risk of pandemic in modern society does not only depend on the pathogen and host characteristics and mode of its transmission, but also on human and environmental factors (population density, population movement, timeliness, and effectiveness of prevention and control measures, as well as ecological changes). Previous studies have shown that population growth, urbanization, global mobility, and changes of the

environment and balance are the main contributing factors associated with the increase of probability of pandemics' occurrence over the past decades [3]. More than 60% of humanity in the 21st century occupy densely populated urban areas [4–6] (Figure 1).

The new infection caused by the severe acute respiratory syndrome coronavirus 2 (SARS-CoV-2) has fulfilled all the conditions to be declared a global threat and to be called a pandemic [7]. In comparison to other coronaviruses and pathogens that have caused outbreaks in the past, COVID-19 is less deadly, but it spreads more easily than the others. The virus's basic reproduction number is higher than that observed for the seasonal influenza. Additionally, the recent studies have shown that railway and aircraft transportation, human mobility (i.e., migrations on all scales), as well as population density significantly correlate with the intensive spread of the novel coronavirus across China and worldwide [8]. As pointed out by the ref. [9] and [10], Geographic Information System (GIS) stands as an essential tool for the analysis of the spatial distribution of infectious diseases and can aid in the process of combating a pandemic and improving the quality of medical care. Since it has an important place in imagery evaluation of disease growth, concentrations variability, or spreading of threats across time, it has much to offer medical geography (health care planning and service provision) and epidemiological research in general. Therefore, mapping the pandemic path presents an important challenge for the humanity. With methods such as interpolation and kriging, GIS can

be of significant assistance to alert others about the COVID-19 spread precisely [9,10]. The understanding of spatial relationships between the pandemic and identifying exposure to the biological hazard in high-risk populations is essential for public health. Hence, GIS is a very important tool in visualization of this data. The spatial data are also helpful in estimating pandemic paths in the geospace [11]. Many methods and techniques supported by GIS could find prominent place in public health and epidemiology research as shown by the contemporary studies conducted worldwide [9–15].

New technologies and mathematical models using known information on population density, population migration patterns, and pathogen transmission capabilities have made it possible to predict and monitor the spread of the disease, the concentration of disease cases, and to identify potential hotspots/epicenters of novel infections [15–17]. Therefore, visualization and modelling of virus paths can help health systems around the world by showing how the virus will continue to spread.

As pointed out by ref. [18], marine, rail, air, and road transport can play dissimilar roles before, during, and after different stages of epidemic outbreaks. Therefore, functions of transportation can be perceived as a dependent, mediating, and moderating variable. The city of Wuhan, in the Chinese Hubei Province, has almost 11 million inhabitants and very frequent air traffic. In 2018, the city's airport registered 20,450,356 passengers [19]. This airport is also the central point between several European and North American airlines (companies). The

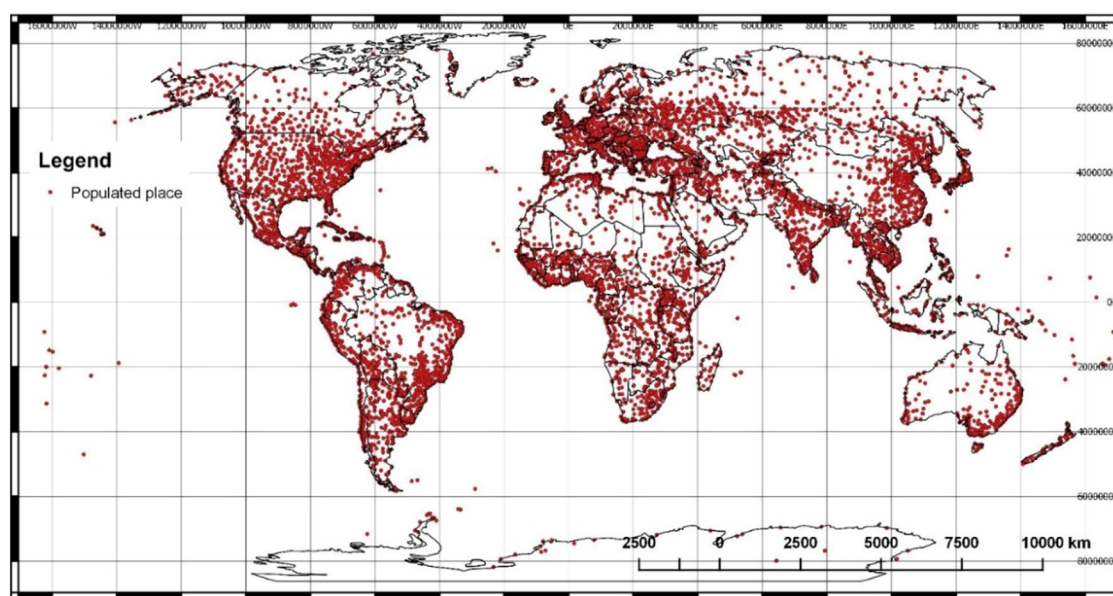


Figure 1: Populated areas of the world.

airport has a huge number of connections between South America, Australia, and Africa, as a stopping point [20]. Previous studies [e.g., ref. 21 and 22] have shown that airplane cabins represent a suitable environment for the transmission of viruses, thus the global increase in new cases of SARS-CoV-2 can be associated with this type of traffic. On the other hand, many people in large cities use more than two types of transportation and commute 40 km daily from home to work and *vice versa*. The most commonly used types of local transportations are trains and buses. However, the highest number of traffic lines worldwide is comprised of air traffic, followed by road traffic, railway traffic, and finally marine traffic [23–25]. In comparison with other types of traffic, air traffic has the highest number of passengers. Even if governments try to mitigate epidemic or pandemic consequences by reducing or stopping traffic, after some time the traffic must be restored again. With restricted population mobility and trade in goods, the global economy tends to fall in recession, which could lead to financial problems, job loss, and expansion of poverty [26]. However, traffic closure is a very important preventive measure for mitigating the virus spread together with quarantine and hygienic methods, as well as reduction of inner and outdoor migrations [27–29]. It is really difficult to control COVID-19 spread without a vaccine, and existing prevention measures cannot be sustained for longer than the next few months. This was especially observed for air traffic, where it was shown that most of the current airport screening measures failed in halting the spread of the virus [22].

2 Materials and methods

2.1 Data source

For the purpose of this study, the data on COVID-19 origin with its geographical dispersion on a global scale throughout the first and second wave was used. Likewise, all vector and raster data of traffic properties and population density on a global scale were included as well. The used data belong to the open source formats. With the help of these data, GIS base was created for mapping and calculations. For that purpose, all populated areas of the world were used in the analysis of the paths of COVID-19 pandemic dispersion [30,31]. The data were taken from the latest United Nations (UN) reports (see Figure 1) and database entitled worldometer (<https://www.worldometers.info/coronavirus/>).

2.2 Pandemic path

As mentioned in the introduction, the first outbreak (case of disease) was identified in Wuhan (Hubei), China. The geographical coordinates of this first point of observation are 30.58°N and 114.28°E. In December 2019, this location was recognized as a cluster of pneumonia cases, where novel coronavirus was eventually identified. Later on, dispersion of COVID-19 was observed in all provinces of China [32–36]. WHO declared the COVID-19 outbreak to be a global public health emergency on 30 January 2020, ranking it at sixth place after the outbreak of H1N1 (2009), Polio (2014), Ebola in West Africa (2014), and Zika (2016) and Ebola in the Democratic Republic of Congo (2019). In the following period, on 11 March 2020, WHO characterized COVID-19 as a pandemic on a global scale [37,38]. In Italy, regions with the most confirmed cases were Bergamo with geographical coordinates 45.7°N/9.6°E and Rome 41.8°N/12.5°E. In the USA, the points with high incidence of cases were New York City 40.6°N/73.9°W; Chicago 41.8°N/87.6°W; Seattle 47.6°N/122.3°W; and Los Angeles 34.05°N/118.25°W. Other places of high concentration of identified cases were Madrid 40.38°N/3.71°W; Barcelona 41.38°N/2.18°E; Berlin 52.52°N/13.40°E; Tehran 35.68°N/51.38°E; Paris 48.85°N/2.35°E; and Bordeaux 44.83°N/0.57°W. These cities represent the main communication and connection points especially regarding the air traffic. More than 40% of the world air traffic in 2019 was located in these airports [39,40] (see Figure 2). These points (airports) are perfectly connected to railway and road networks. They have huge population density, higher than 500 inhabitants per 1 km². Due to all elements listed above, the COVID-19 virus is well-dispersed on all sides of the world, excluding Antarctica.

According to ref. [41], air transport has created its own vulnerabilities during the years, because it is a vector in the spread of pathogens and diseases on various scales. This was confirmed by the latest pandemic worldwide situation regarding COVID-19 where airports and aircrafts act as potential incubators and nodes of disease distribution (Figure 2). The mentioned facts should push worldwide states to take radical structural actions to deal with these emergencies in the future with the ongoing pandemic.

2.3 Mathematical background of COVID-19 paths

In this study, we calculated two potential paths of COVID-19. These paths are actually two types of distribution. First, we presented the worst scenario in case of pandemic wave



Figure 2: Frequencies of airplane lines in 2019 – the main corridor is between Mainland China, Western Europe, and the USA. This map was generated using open source GIS software QGIS; the data were taken from the International Air Transport Association.

occupying the whole world. In that case, we can expect exponential growth of pandemic spread (see equation (1)).

$$P(X = x) = \frac{e^x \cdot e^{-u}}{x!} \quad (1)$$

Equation (1) presents modified exponential distribution or Poisson distribution. X is the Poisson distribution with mean u . This distribution is better than classic exponential distribution because the parameter of measure m depends on the average time between occurrences. In our case, that presents the start of pandemic and current pandemic situation. This close exponential distribution is very useful for calculations in natural science and medicine [42].

Another distribution used and elaborated in this research is geometric. This distribution presents the current stage of the pandemic since the humanity is still waiting for the vaccine. This distribution could be presented in the following form (see, e.g., 2-equation (4)).

$$P(X = x) = q^{(x-1)}p \quad (2)$$

where

$$E(x) = 1/p \quad (3)$$

$$\text{Var}(x) = q/p^2, q = 1 - p \quad (4)$$

This dispersion is very useful because the results could be used for GIS calculations.

2.4 GIS analysis of pandemic paths at global scale

With the help of spatial information tool such as GIS and algorithms used in this research, potential scenarios of

virus distribution on a global scale were modelled. As pointed out by the ref. [9], spatial models are fundamental tools to statistically investigate the geographic relationship between several explanatory variables and disease outbreak such as COVID-19. This is why GIS has become an important tool in analyzing and visualizing the spread of COVID-19, regardless of the fact that a limited number of GIS-based studies have been published since the initial outbreak. The analyzed data for the purpose of this study included air, railway, marine, and road traffic. Due to the fact that there are numerous models of possible trajectory of viruses, in this research the authors used classical GIS and advanced numerical methods. With the usage of two software's QGIS 3.12. (Quantum Geographical Information System) and GRASS GIS, analysis and estimation of traffic capacities, as well as virus paths across the globe were investigated. All the procedures and all the algorithms used for the purpose of this research were presented in the flow chart (see Figure 3), which was modified in a way to point out the algorithm of spatial analysis of COVID-19 dispersion across the world.

For the analysis of potential dispersion of COVID-19 on a global scale, conventional models were used. The first presented model is extreme and it uses exponential progression. It is marked as dangerous potential of COVID-19 for dispersion across the world. The second model is used to assess medium and mild increase of pandemic cases across the world and it uses geometric progression for the analysis of COVID-19 dispersion. By using special GIS numerical methods, spatial properties at the time of the beginning of the spread of the virus were reconstructed.

As already pointed out, GIS and modelling of pandemic data can be very powerful tools for calculating and describing some major properties of COVID-19.

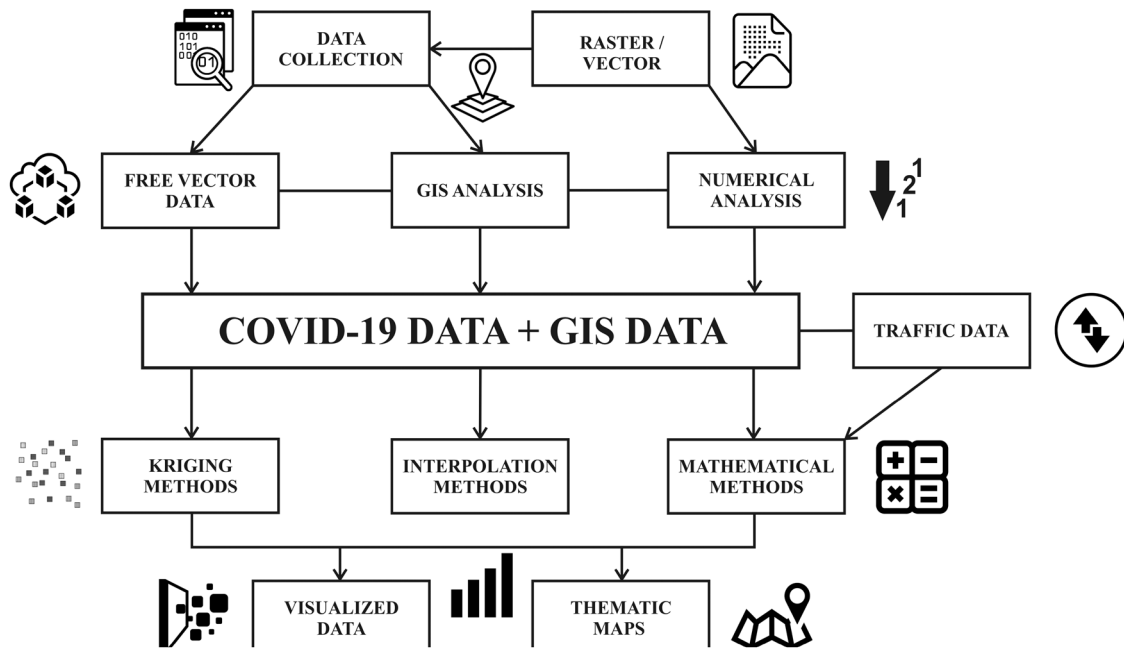


Figure 3: Algorithms and procedures used in this research.

GIS software QGIS and SAGA (System for Automated Geoscientific Analyses), along with the tools for geospatial calculations, were used for the visualization of the infected cases dispersion across the world. The ordinary and semi-kriging methods were used through QGIS and SAGA (GIS) of the Spatial Analyst. Other methods used include interpolation and semi-zonal algorithms. The number of virus-infected cases over certain area depends on the density of population which is important for future predictions. By using QGIS within heat map layer, the zones of the virus dispersion were observed [43,44]. The traffic networks were created in open source software Gephi 0.9.1. This software was used for quantification and analysis of graph properties for all types of traffic. For each traffic network, the modified Likert scale in QGIS was applied. The results are given between 0.0 (the lowest result) and 1.0 (the best result). Beside the Likert scale, in this research, the authors used analysis of network properties by applying the buffer and threshold ring analysis [45]. Two types of buffers were used: (a) rounded buffer with radius of 20; 50; and 100 km – used for the analysis of railroads and roads, and (b) circular buffer of 20; 50; and 100 km – used for the analysis of ports. In the final phases, correlation method was used. This method connected two types of values y and x , while r is the coefficient of correlation between y and x . The value of r can vary between -1 and $+1$, where $r = 1$ indicates that an increase in x is associated with a corresponding increase in y , $r = -1$ indicates that an increase in x is

associated with a corresponding decrease in y , and $r = 0$ indicates the absence of a predictable relationship. The main formula used for this purpose has the following form (equation (5)):

$$r = \frac{\sum_{i=1}^n (x_i - \bar{x})(y_i - \bar{y})}{\sqrt{\sum_{i=1}^n (x_i - \bar{x})^2 \times \sum_{i=1}^n (y_i - \bar{y})^2}} \quad (5)$$

where the value r is a summary measure relating to an entire set of paired observation. In this research, the r was varied between 0.1; 0.3; and 0.6 [46,47]. Other GIS methods used in this research encompassed semi-automatic spatial analysis, buffer analysis, visualization of raster objects, categorization, and graduation.

3 Results

From the airplane traffic network, it can be seen that the total path length of all airplane lines in 2019 was 4.1×10^{15} km. The largest number of lines is between America and Europe 37%, then between Asia and Europe 33%, North America and South America 11%, Asia and East Asia 9%, Europe and Africa 5%, and other 5%. The total number of nodes (airports) is 5,623; the total number of edges is 72,406 (number represents the trajectory of direct airplane lines). The results in modified Likert scale are: the mobility of air traffic is 1.0; the connectivity is 0.6; the availability is 0.8; the density of graph which

represents direct lines is 0.002; the modularity is 0.0; the average clustering coefficient is 0.270; and the centrality is 0.03. The number of weekly connected lines is 2,206 and the number of frequent lines is 2,242. In the USA, the biggest node is Atlanta's airport; in Europe, the biggest nodes are identified in the UK (Heathrow), in Germany (Frankfurt Airport), in Netherland (Schiphol), in France (Charles De Gaulle), and in Turkey (New International Airport). In Central Asia, the biggest nodes are Sheremetyevo in Russia, Beijing Capital International Airport, and Shanghai Pudong International Airport.

The results of the modified Likert scale of the road traffic networks are: the mobility of road traffic is 0.8, the connectivity is 1.0, and the availability 0.7. The densest road network is located in the eastern part of the USA, western and central part of Europe, and on the east coast of China. The road traffic network between three continents, i.e., between North and South America across the Central America, is a closed network. The number of possible connected lines is 1.5×10^9 per month (see Figure 4c and Table 1).

The roads of Europe, Asia, and Africa belong to the same closed network. The highest number of possible connected lines per month is in Europe (2.3×10^9).

This graph (network) for all continents has the following characteristics that can be observed in Table 1.

Table 1: Properties of road network in the world

| Continent | Centrality | Clustering coefficient | Modularity | Connectivity |
|---------------|------------|------------------------|------------|--------------|
| Europe | 0.06 | 0.420 | 0.2 | High |
| North America | 0.07 | 0.340 | 0.1 | High |
| South America | 0.05 | 0.690 | 0.4 | Moderate |
| Asia | 0.09 | 0.770 | 0.5 | Moderate |
| Australia | 0.08 | 0.620 | 0.3 | Moderate |
| Africa | 0.06 | 0.560 | 0.6 | Low |
| Antarctica | 0.09 | 1.000 | 1.0 | Very low |

The road networks in Australia and East Asia are isolated. The number of possible connected lines per month in Australia is 0.4×10^9 . In Asia, the number of possible connected lines per month is 5.2×10^9 . In South America, the number of possible connected lines per month is 2.6×10^9 .

The railway traffic network has the following results: the mobility is 0.9; the connectivity is 0.3; and the availability is 0.9. The railway graph is relatively less connected in comparison with road graph. The railways traffic network in North America represents the

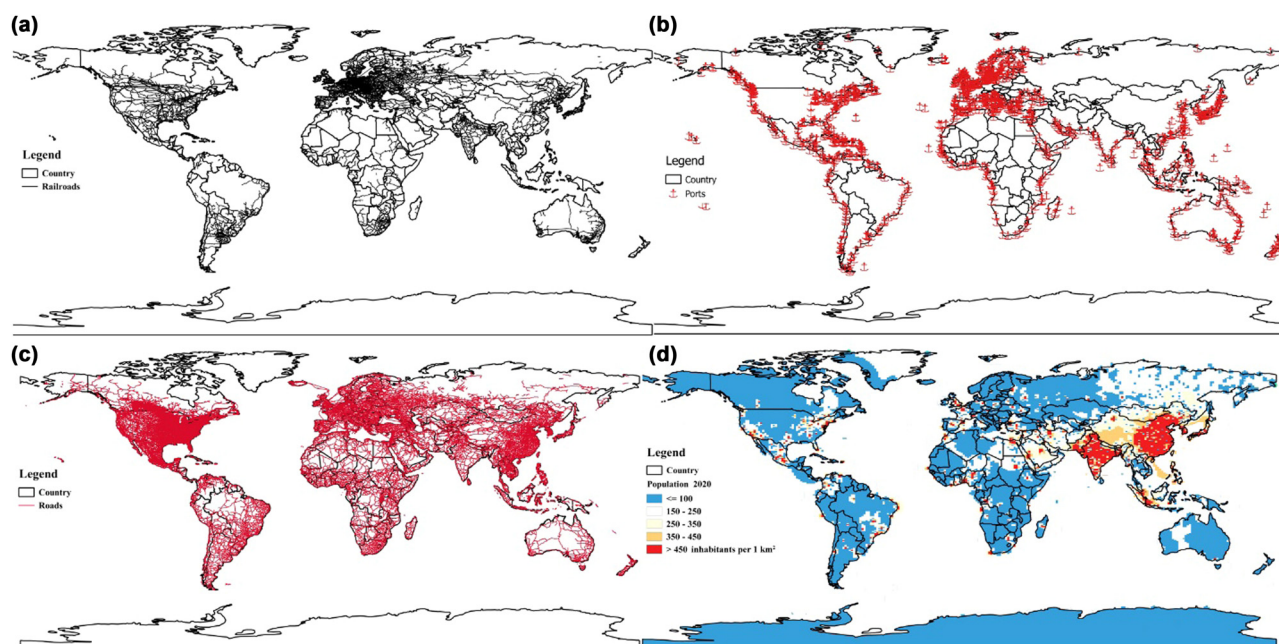


Figure 4: Traffic networks and population density on a global scale; (a) railway network is the densest in Europe; (b) ports are highly distributed in Western Europe and the East of USA; (c) the longest roads with the highest density are in the USA and Europe; (d) according to the UN data, the highest population density is in Western Europe, east coast of the USA, Central America, east coast of South America, east coast of Central Africa, North India, South-east Asia, southeast coast of Australia, and Japan. These maps were created with the help of open source GIS software.

Table 2: Properties of railway network in the world

| Continent | Centrality | Clustering coefficient | Modularity | Connectivity |
|---------------|------------|------------------------|------------|--------------|
| Europe | 0.03 | 0.210 | 0.2 | High |
| North America | 0.03 | 0.270 | 0.3 | High |
| South America | 0.09 | 0.770 | 0.8 | Low |
| Asia | 0.06 | 0.555 | 0.5 | Moderate |
| Australia | 0.08 | 0.778 | 0.7 | Moderate |
| Africa | 1.1 | 0.989 | 0.9 | Low |
| Antarctica | — | — | — | Very low |

dependent graph. The number of possible connected lines per month is 1.3×10^3 .

The railway graph has the following characteristics: the modularity is 0.4; the average clustering coefficient is 0.370, and the centrality is 0.05 (see Figure 4a and Table 2).

The number of possible connected lines per month in South America is 0.9×10^2 . Europe has the largest railway network and the number of possible connected lines per month is 2.8×10^4 . In railways of Asia, the number of possible connected lines per month is 0.7×10^3 (see Table 2).

The results of the marine traffic network are: the mobility is 0.2, the connectivity 0.1, and the availability 0.4. As it can be seen on Figure 4b, ports are highly distributed in Western Europe and the East of USA.

After digitizing the population density data, the results of average density of regions on a global scale excluding the oceans were obtained. The average density in 2019 was 52 inhabitants per 1 km^2 . The highest density is in North India, Central and Western Europe, east coast of the USA, west coast around San Francisco, east coast of China, central part of China, southeast part of Australia, conurbations in Japan, and the biggest cities in Africa and South America, where there is more than 100 inhabitants per 1 km^2 (see Figure 4d). These data are supported by the densest traffic networks of roads, railways, and large airports (Figure 4). It is easy to point out that during pandemic these areas are the most susceptible to infection spreading.

The railroad network shows 33×10^7 vertices at global scale. When buffer analysis was performed, three radius belts were derived. First one represents belt with 20 km radius (see Figure 5a). This belt covers vast areas in Europe, the countries like Germany, France, Italy, Austria, Spain, Portugal, Great Britain, Switzerland, Belgium, Netherlands, Poland, Slovakia, Czech Republic, Hungary,

Bulgaria, Greece, etc. On the second place regarding the network density is the United States of America, followed by India, South America, South-east Australia, and Central and Eastern China. The belts of 50 km radius possess connectivity that is very similar to the first belt; with zones expanding on 50 more countries (see Figure 5b). Finally, the belts with a radius of 100 km cover >35% areas than first two belts. This belt encompasses +76 countries more than first belt. This largest belt is closely linked with huge urban areas. Also, it elongates closely with road networks (see Figure 5c).

The total capacity of roads at global scale is 56×10^9 vertices. After finalization of buffer analysis, the three belts of 20 km (A), 50 km (B), and 100 km (C) showed prominent feature for potential dispersion of COVID-19 regarding the road traffic networks (see Figure 6a–c).

Road networks display a far better possibility for COVID-19 dispersion because it is fifty times denser in comparison with the railroad network. The east coast of the United States of America has a high connectivity and high potential of traffic flow. The following regions and countries exhibit the similar results: Western Europe, South-east Europe, South East China, Japan, Central America, South Africa, South-east Australia, and all areas close to big agglomerations. The first belt with a radius of 20 km has high potential in the eastern parts of the United States of America and Western Europe due to possible connectivity with other types of traffic. The belt of 50 km covers the same areas, and it extends on the +90 countries across the world. Ninety percent of areas near big cities belong to this belt. Finally, the belt of 100 km radius encompasses 199 countries and territories, covering 75% of the world. This belt has higher risk of susceptibility to COVID-19 dispersion via road traffic. Only areas in Antarctica, Central Australia, Greenland, Northern Canada, Arctic Circle, Central and Eastern parts of Russian Federation, and Central parts of the Amazon Basin are likely to be unaffected. This belt has a good possibility for connection with all traffic types. In that way, COVID-19 is more likely to be dispersed via roads, rather than railroads network (5 times faster with 40% larger area).

3.1 Modelling and mapping of COVID-19-spreading paths

In this study, all countries in the world affected by the COVID-19 were analyzed. According to the availability of

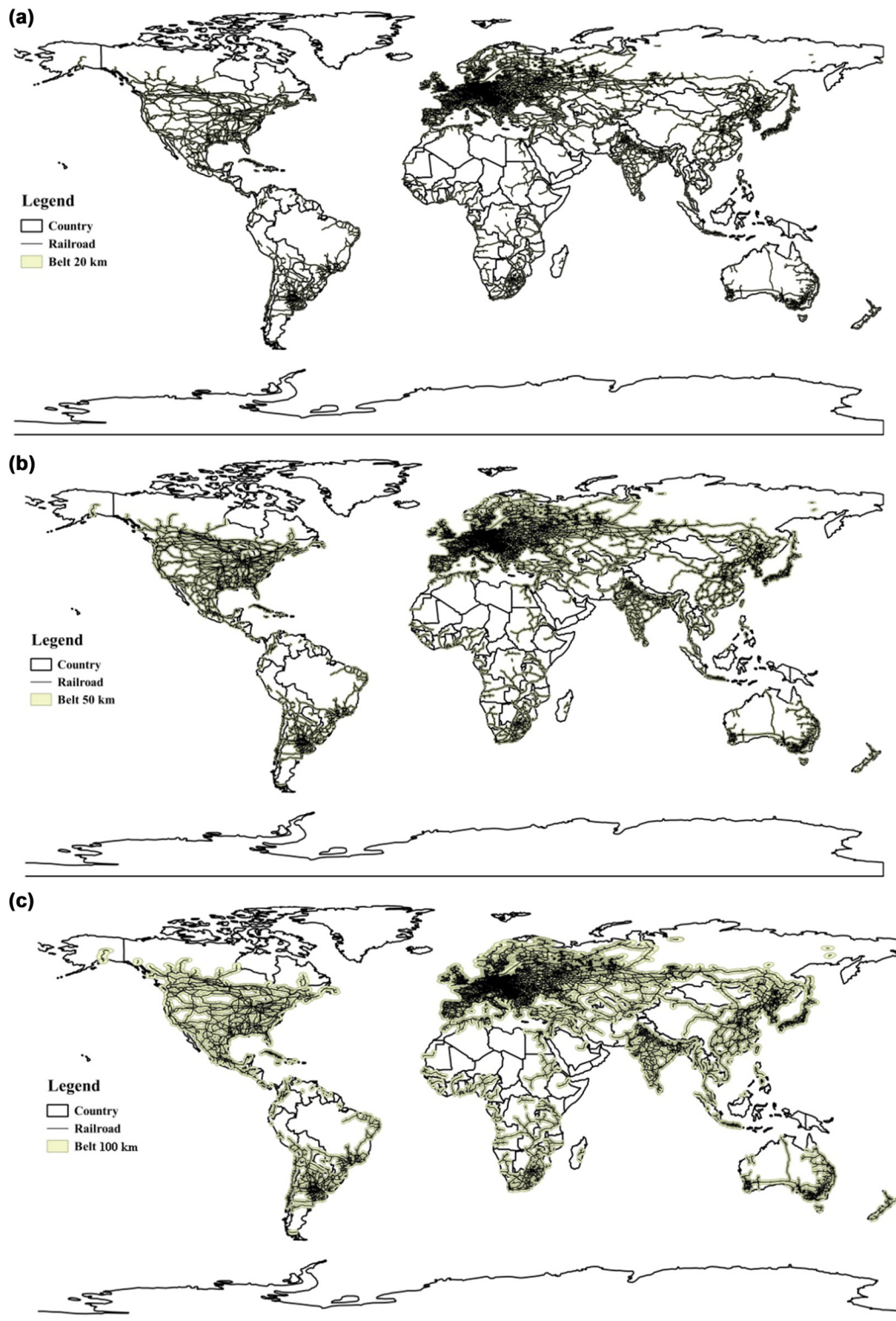


Figure 5: Buffer analysis of railroads of potential three belts with a radius of 20 km (a); 50 km (b); and 100 km (c) at global scale.

new data, trajectory of virus-spreading paths was estimated. It was observed that in the present conditions on a global scale, the expansion rate of virus is very

similar to geometric progression. For all estimated cases, two other types of progression, arithmetic and exponential, were used. After modelling and mapping of the

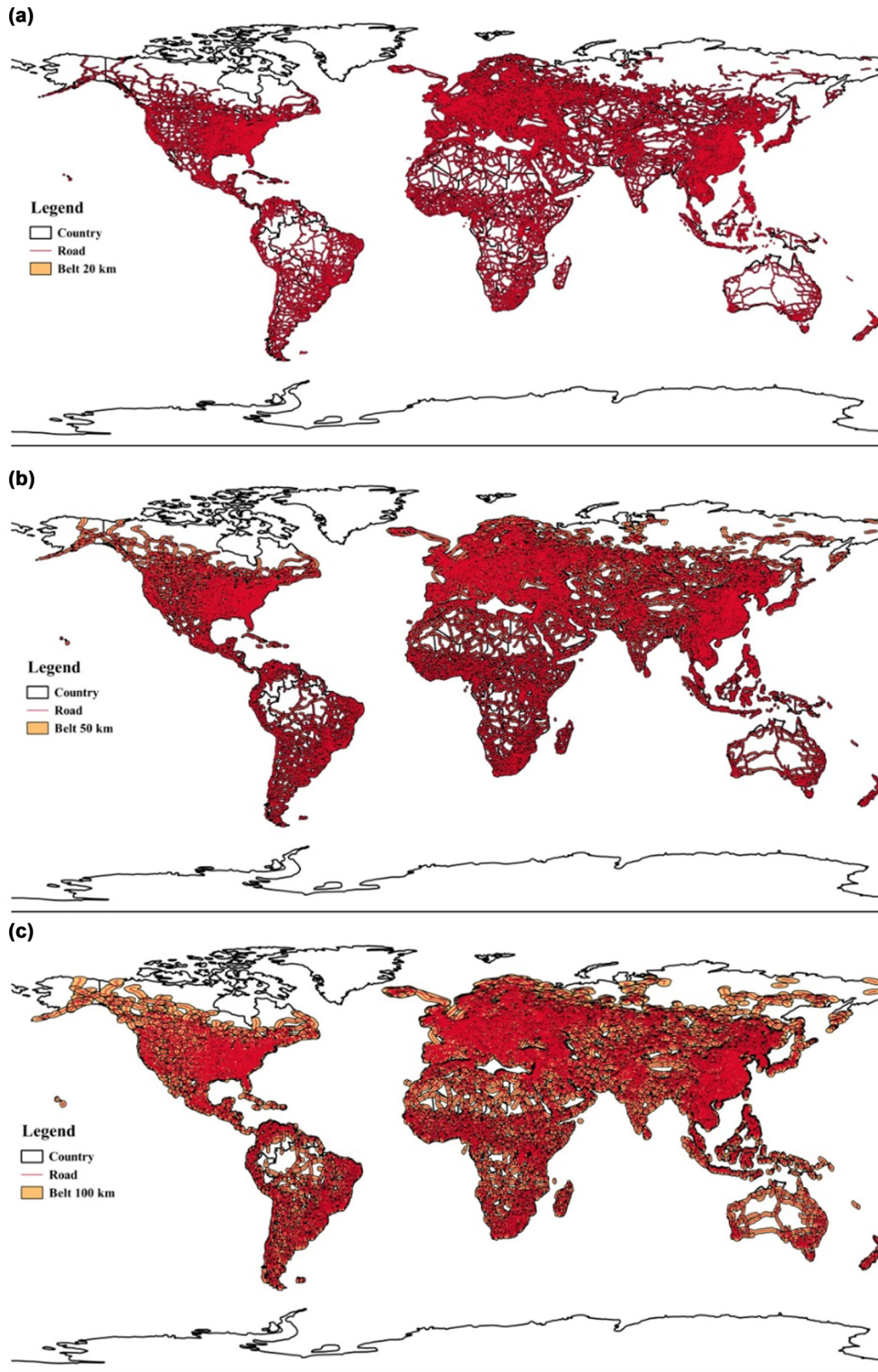


Figure 6: Buffer analysis of roads of potential three belts with a radius of 20 km (a); 50 km (b); and 100 km (c) at global scale.

results on a global scale, it was observed that the pandemic dispersion (between the first two waves) shifted toward the USA and Europe (Figure 7a and b). The large

and densely populated areas in the USA and Europe, the areas of big conurbations with large infrastructure of traffic networks, will be more affected and susceptible

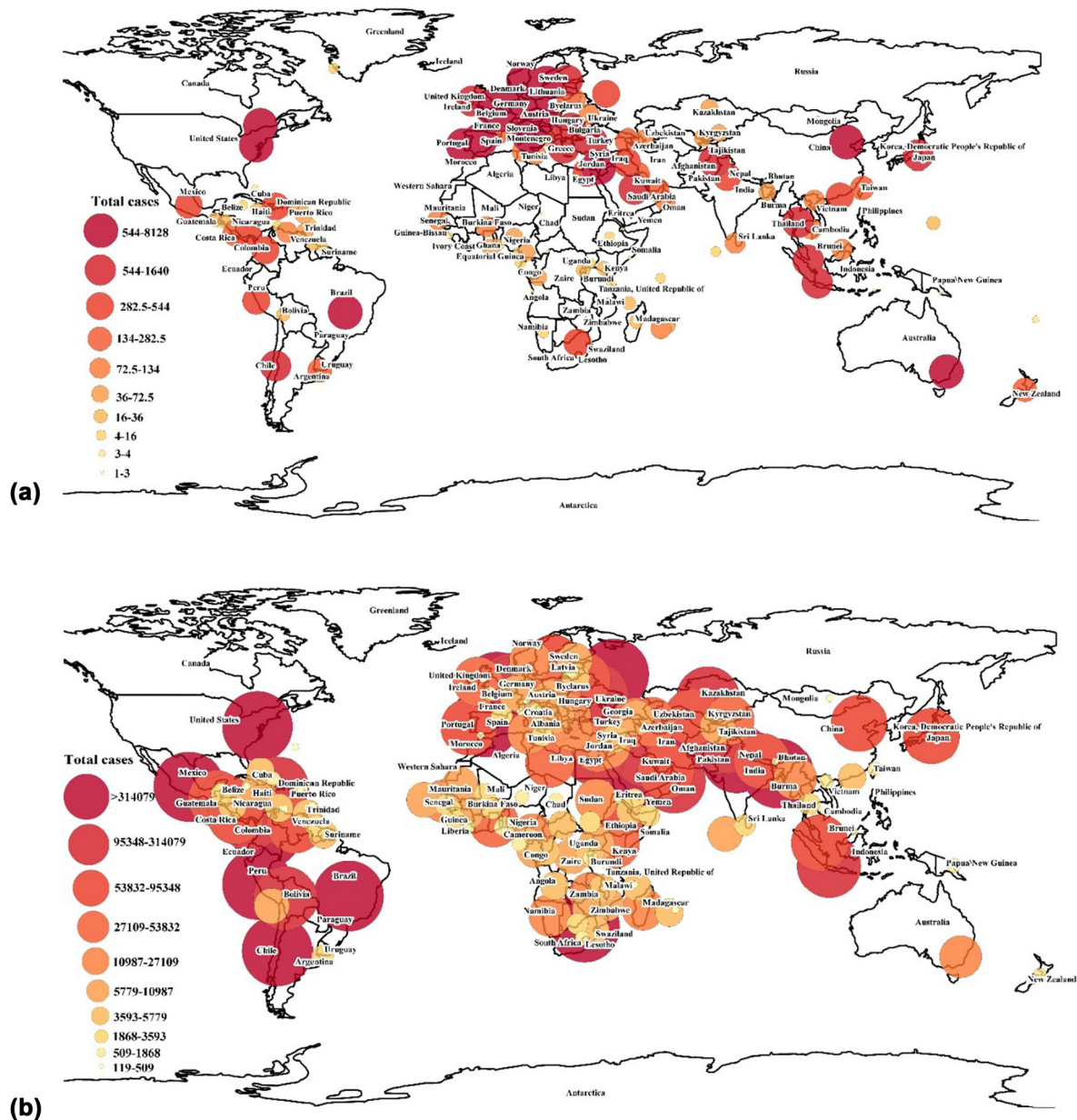


Figure 7: (a) The beginning of pandemic with geographical dispersion of first reported cases across the world (for pandemic visualization, the capital city of all countries and territories was used). (b) The contemporary situation of pandemic includes the rapid acceleration of reported cases across the world.

to the COVID-19. Only sparsely populated areas with underdeveloped and small traffic networks (and isolated island territories) will be less or not affected (see Figure 7a and b). From these figures, potential COVID-19 dispersion with included geometric progression was analyzed. Hence, it can be observed which areas are more likely to be affected by the ongoing COVID-19 pandemic. Dispersion belts (between first and second wave) can be observed after thorough GIS analysis (Figure 7a and b). From the Figure 7b, it can be observed that, during the

contemporary pandemic situation, more than 213 countries and territories are affected by COVID-19. The first belt with a high percentage of reported cases covers areas with frequent traffic and dense population, encompassing the big agglomerations across the world. It stretches over Brazil, Chile, Columbia, and Peru in South America, Mexico in Central America, and the USA in North America. In Europe, this belt stretches over territories of Spain, Italy, France, and Great Britain. In Eurasia, the belt encompasses the Russian Federation,

Turkey, Iraq, Iran, Saudi Arabia, and Bangladesh. Republic of South Africa dominates in the African continent in terms of total registered cases. The belt with low registered cases includes Tanzania, Comoros, Faeroes Islands, Gibraltar, Saint Martin, Mauritius, Eritrea, Mongolia, North Korea, Cambodia, Monaco, Bhutan, Barbados, Brunei, and Liechtenstein. Other countries and territories belong to the medium belts regarding the reported cases (see Figure 7b). The other territories which would be affected by the ongoing pandemic situation are agglomerations in the South-East Asia and East Australia.

4 Discussion

From the Figure 7a and b, it is possible to observe the change of COVID-19 dispersion on a global scale. This represents the medium scenario of virus progression. In this scenario, the infected cases encompass >200 countries and territories. With the new dispersion belts identified in the USA and Europe, the virus tends to spread to other border territories. In the worst prediction model scenario, where exponential progression is used, the number of infected cases ranges between 60 and 70% of the world population [48–50]. In the analysis of traffic network dispersion and density, it is important to point out that air traffic is more dangerous regarding the infection spread than road, railway, and marine traffic. The largest and most densely populated areas in the USA, such as New York, Chicago, Indianapolis, California, Arizona, Vermont, New Jersey, Ohio, New Orleans, and Indiana, will be strongly affected according to the presented model results. The isolated and low population density states, such as Idaho, Montana, Wyoming, North Dakota, South Dakota, and Alaska, are expected to be less affected. In Europe, countries in Scandinavia and small islands in the Atlantic Ocean including Greenland will most likely be less affected. The Asian part of Russian Federation has low population density and undeveloped road and railway traffic networks, so it will also probably be less affected. Siberia and the countries in Central Asia will most likely experience a small number of virus-infected cases. Central part of South America and central part of Canada will most likely be less affected as well, due to low population density and poorly developed traffic networks.

The contemporary studies indicate that since January, the virus has rapidly spread over the world, with significant outbreaks occurring in countries such as Italy, Iran, Brazil, and the United States of America. As of June 30th,

there were cumulatively 26,18,817 cases and 1,26,623 death cases associated with COVID-19 in the USA according to ref. [51]. Also, ref. [52] obtained results which indicate that a spatial ordinary least squares regression model tends to overestimate the COVID-19 period prevalence among counties in the United States. On the other hand, respective authors outline that spatial models can better estimate the period prevalence for counties, especially along the Atlantic coasts and through the Black Belt.

In Europe, study of [53] shows that up to 80% of the UK population have been infected, with a total of more than 3,00,000 cases and 42,000 associated deaths being announced as of 22nd June 2020. On the other hand, study of [54] emphasizes that the impact of COVID-19 pandemic on the Finnish society has been somewhat unpredictable, although it has not been as extensive and massive as in other European countries. Respective authors state that by August 2020, the reported number of COVID-19 cases rose up to 7,464 and the number of deaths up to 333 with recovery rate over 90% of all reported cases. Contemporary studies of novel corona virus in East Asia (China) report 80,793 confirmed cases and 3,169 deaths on the Chinese mainland from March onward [55,56]. The study of [57] points out that for India (in the region of South Asia), the overall volume of infected cases is definitely less compared to other countries due to timely announcement of lockdown and considerable efforts invested by Indian authorities to impose stringent lockdown. Also, the authors discuss that Indian Railways have come up with an innovative approach by converting train coaches into health care facilities if a situation arises with large volumes of infected cases due to the importance of this type of public transport across the country. In the region of Middle East, Iran became the second focal point of COVID-19 in the world after China virus outbreak. According to [58] (2020), until April 14, 74,877 cases have been identified in the country, of which 4,683 (6.25%) have died. The African continent reported 12,37,070 cases, 29,430 deaths, and 9,68,962 recoveries. Republic of South Africa has experienced severe infection outbreak with highest cumulative COVID-19 cases and accounts for 90% of the confirmed deaths, with fatality ratio of 7% [59]. Observed case studies over the world correspond quite well with the obtained dispersion belts (between first and second wave) generated through GIS analysis (Figure 7a and b). The main advantage of GIS methods in this investigation lies in easy analysis of geospatial data and in the possibility to visualize these data. The error of GIS analysis used in this research varied between 0.5 and 1.0%.

The buffer and interpolation models outline that GIS techniques, resources, and methods can be efficiently used for more effective investigation of vulnerable geographical locations around the world. Also, geographic modelling of COVID-19 distribution on global scale can provide useful insights for policymakers (for targeted interventions) and for authorities in order to identify the highly affected areas and take appropriate actions. This emphasizes the significance of utilization of GIS techniques and adequate interpretation of geospatial information for understanding the spatiotemporal dynamics of COVID-19 and its mitigation, as well as sustainable health care management in different parts of the world.

5 Conclusion

In the long history of mankind, the pandemic always presents one of the biggest threats to the entire world population. Other threats for the world population are associated with economic problems and everyday living necessities. In this research, it was noted that air traffic has high share regarding the mobility, especially in the USA and Europe, as well as in Mainland China. The connectivity with other traffic networks is ranked as average – it is better with the road traffic system, and less with railway traffic. The reason for this lies in the fact that speed of air traffic is relatively high, some lines even have reconnections. Road traffic has high mobility, the highest connectivity, and reliable availability. This is due to the fact that road traffic can operate “door to door.” Other traffic such as marine does not present real threat to humanity during pandemic, because ports can be very easily quarantined. These scenarios were compared with population density accompanied with the data from 2019. Four types of traffic were investigated in conjunction with pandemic dispersion of COVID-19. Obtained results highlight that mobility, connectivity, and availability of traffic resources can be crucial in the analysis of virus-spreading paths. The worldwide pandemic is ongoing and the model derived areas with high and low dispersion of COVID-19. For the worst prediction model, where exponential progression is used, the number of infected cases spans between 60 and 70% of world population. This requires important measures that need to be addressed and implemented in order to successfully mitigate the implications of COVID-19 not only on global, but also on local and regional scales. There are a number of limitations in this

research. Although authors investigated the influence of different types of traffic on human mobility and thus dispersion of infection on global scale, future studies should be oriented towards a more comprehensive analysis of the detailed impact of different travel types on the pandemic. Therefore, future studies are recommended to be more focused on the assessment of the volume of air travel, as well as on the investigation of the impact of sea, bus, train, and car travels (with usage of daily, monthly, and yearly data resolution) on the distribution of COVID-19 in different regions of the world. Also, necessity for unique geodatabase which would comprise environmental, socio-economic, topographic, and demographic variables should be imperative for some future work that would strive to explain the spatial variability of disease incidence. For this purpose, artificial intelligence-driven methods can be useful to predict the parameters, risks, and effects of such a pandemic, which would be crucial for COVID-19 mitigation measures that could be implemented in many regions of the world.

Acknowledgments: Authors are grateful to the anonymous reviewers whose constructive comments and suggestions greatly improved the manuscript.

References

- [1] Madhav N, Oppenheim B, Gallivan M, Mulembakani P, Rubin E, Wolfe N. Pandemics: Risks, impacts, and mitigation. In: Jamison DT, Gelband H, Horton S, et al., editors. *Disease control priorities: Improving health and reducing poverty*. 3rd edn. Washington (DC): The International Bank for Reconstruction and Development/The World Bank; 2017. Chapter 17. Available from: <https://www.ncbi.nlm.nih.gov/books/NBK525302/>.
- [2] Raoult D, Zumla A, Locatelli F, Ippolito G, Kroemer G. Coronavirus infections: Epidemiological, clinical and immunological features and hypotheses. *Cell Stress*. 2020;4(4):66–74. doi: 10.15698/cst2020.04.216.
- [3] Zhu L, Zhang C, Zhang C, Zhang Z, Nie X, Zhou X, et al. Forming a new small sample deep learning model to predict total organic carbon content by combining unsupervised learning with semisupervised learning. *Appl Soft Comput*. 2019;83:105596.
- [4] MacPherson DW, Gushulak BD, Baine WB, Bala S, Gubbins PO, Holtom P, et al. Population mobility, globalization, and antimicrobial drug resistance. *Emerg Infect Dis*. 2009;15(11):1727–31. doi: 10.3201/eid1511.090419.
- [5] Antrop M. Landscape change and the urbanization process in Europe. *Landscape change and the urbanization process in Europe*. *Landscape Urban Plan*. 2004;67:9–26. doi: 10.1016/S0169-2046(03)00026-4.

- [6] Dadao LU. Urbanization process and spatial sprawl in China. Ontario: Urban Planning Forum; 2007; Robinson AH, Morrison JL, Muehrcke PC, Kimerling JA, Guphill SC. Elements of Cartography. 6th edn. Hoboken: John Wiley and Sons; 1995.
- [7] Song E, Yoo HJ. Impact of social support and social trust on public viral risk response: A COVID-19 survey study. *Int J Environ Res Public Health*. 2020;17:6589. doi: 10.3390/ijerph17186589.
- [8] WHO. Director-General's opening 7 remarks at the media briefing on COVID-19 – 11 March 2020. World Health Organization; 11 March 2020. Accessed date: 24 March 2020.
- [9] Mollalo A, Vahedi B, Rivera KM. GIS-based spatial modeling of COVID-19 incidence rate in the continental United States. *Sci Total Environ*. 2020;728:138884. doi: 10.1016/j.scitotenv.2020.138884.
- [10] Sarwar S, Waheed R, Sarwar S, Khan A. COVID-19 challenges to Pakistan: Is GIS analysis useful to draw solutions? *Sci Total Environ*. 2020;730:139089. doi: 10.1016/j.scitotenv.2020.139089.
- [11] Nykiforuk CIJ, Flaman LM. Geographic information systems (GIS) for Health Promotion and Public Health: A review. *Health Promot Pract*. 2011;12(1):63–73. doi: 10.1177/1524839909334624.
- [12] Guo D. Visual analytics of spatial interaction patterns for pandemic decision support. *Int J Geograph Inf Sci*. 2007;21(8):859–77. doi: 10.1080/13658810701349037.
- [13] Zhang L, Yang H, Wang K, Zhan Y, Bian L. Measuring imported case risk of COVID-19 from inbound international flights – a case study on China. *J Air Transp Manag*. 2020;89:101918. doi: 10.1016/j.jairtraman.2020.101918.
- [14] Schröder W. GIS, geostatistics, metadata banking, and tree-based models for data analysis and mapping in environmental monitoring and epidemiology. *Int J Med Microbiol*. 2006;296(S1):23–36.
- [15] Zhou C, Su F, Pei T, Zhang A, Du Y, Luo B, et al. COVID-19: Challenges to GIS with Big Data. *Geogr Sustainability*. 2020;1:77–87. doi: 10.1016/j.geosus.2020.03.005.
- [16] Christaki E. New technologies in predicting, preventing and controlling emerging infectious diseases. *Virulence*. 2015;6(6):558–65. doi: 10.1080/21505594.2015.1040975.
- [17] Centers for Disease Control and Prevention. The Deadliest Flu: The Complete Story of the Discovery and Reconstruction of the 1918 Pandemic Virus. Atlanta: National Center for Immunization and Respiratory Diseases (NCIRD); 2019. Available from: <https://www.cdc.gov/flu/pandemic-resources/reconstruction-1918-virus.html>.
- [18] Li Q, Guan X, Wu P, Wang X, Zhou L, Tong Y, et al. Early transmission dynamics in Wuhan, China, of novel coronavirus-infected pneumonia. *N Engl J Med*. 2020;382(13):1199–207. doi: 10.1056/NEJMoa2001316.
- [19] <https://www.iata.org/> (accessed on 22.05.2020).
- [20] Han X, Naeher LP. A review of traffic-related air pollution exposure assessment studies in the developing world. *Environ Int*. 2006;32:106–20. doi: 10.1016/j.envint.2005.05.020.
- [21] Jones KE, Patel NG, Levy MA, Storeygard A, Balk D, Gittleman JL, et al. Global trends in emerging infectious diseases. *Nature*. 2008;451(7181):990–3. doi: 10.1038/nature06536.
- [22] Morel Sokadjo Y, Atchadé MN. The influence of passenger air traffic on the spread of COVID-19 in the world. *Transport Res Interdiscip Perspect*. 2020;8:100213. doi: 10.1016/j.trip.2020.100213.
- [23] Callaway E, Cyranoski D, Mallapaty S, Stoye E, Tollefson J. The coronavirus pandemic in five powerful charts. *Nature*. 2020;579(7800):482–3. doi: 10.1038/d41586-020-00758-2.
- [24] Prem K, Liu Y, Russell TW, Kucharski AJ, Eggo RM, Davies N. The effect of control strategies to reduce social mixing on outcomes of the COVID-19 epidemic in Wuhan, China: A modelling study. *Lancet Pub Health*. 2020;5:e261–e270. doi: 10.1016/S2468-2667(20)30073-6.
- [25] Kistemann T, Dangendorf F, Schweikart J. New perspectives on the use of Geographical Information Systems (GIS) in environmental health sciences. *Int J Hyg Environ Health*. 2002;205(3):169–81. doi: 10.1078/1438-4639-00145.
- [26] Tim US. The application of GIS in environmental health sciences: Opportunities and limitations. *Environ Res*. 1995;71(2):75–88. doi: 10.1006/enrs.1995.1069.
- [27] Guo D. Visual analytics of spatial interaction patterns for pandemic decision support. *Int J Geograph Inf Sci*. 2007;21(8):859–77. doi: 10.1080/13658810701349037.
- [28] Dong E, Du H, Gardner L. An interactive web-based dashboard to track COVID-19 in real time. *Lancet Infect Dis*. 2020;20(5):533–4. doi: 10.1016/S1473-3099(20)30120-1.
- [29] Wu ST, Chen YS. Examining eco-environmental changes at major recreational sites in Kenting National Park in Taiwan by integrating SPOT satellite images and NDVI. *Tour Manag*. 2016;57:23–36. doi: 10.1016/j.tourman.2016.05.006.
- [30] Biscayart C, Angeleri P, Lloveras S, Do Socorro Souza Chaves T, Schlagenhauf P, Rodriguez-Morales AJ. The next big threat to global health? 2019 novel coronavirus (2019-nCoV): What advice can we give to travellers? – Interim recommendations January 2020, from the Latin-American society for Travel Medicine (SLAMVI). *Travel Med Infect Dis*. 2020;33:101567. doi: 10.1016/j.tmaid.2020.101567.
- [31] Wilson ME. What goes on board aircraft? Passengers include Aedes, Anopheles, 2019-nCoV, dengue, Salmonella, Zika, et al. *Travel Med Infect Dis*. 2020;33:101572. doi: 10.1016/j.tmaid.2020.101572.
- [32] Bai Y, Yao L, Wei T, Tian F, Jin DY, Chen L, et al. Presumed asymptomatic carrier transmission of COVID-19. *JAMA*. 2020;323(14):1406–7. doi: 10.1001/jama.2020.2565.
- [33] Gumel AB, Ruan S, Day T, Watmough J, Brauer F, Van den Driessche P, et al. Modelling strategies for controlling SARS outbreaks. *Proc R Soc B Biol Sci*. 2004;271:2223–32.
- [34] Rabi FA, Al Zoubi MS, Kasasbeh GA, Salameh DM, Al-Nasser AD. SARS-CoV-2 and coronavirus disease 2019: What we know so far. *Pathogens*. 2019;9:231. doi: 10.3390/pathogens9030231
- [35] Pan F, Ye T, Sun P, Gui S, Liang B, Li L, et al. Time course of lung changes on chest CT during recovery from novel coronavirus (COVID-19) pneumonia. *Radiology*. 2020;295:715–21. doi: 10.1148/radiol.2020200370.
- [36] Liu Y, Gayle AA, Wilder-Smith A, Rocklöv J. The reproductive number of COVID-19 is higher compared to SARS coronavirus. *J Travel Med*. 2020;27:1. doi: 10.1093/jtm/taaa021.
- [37] Rabi FA, Al Zoubi MS, Kasasbeh GA, Salameh DM, Al-Nasser AD. SARS-CoV-2 and coronavirus disease 2019: What

- we know so far. *Pathogens*. 2019;9:231. doi: 10.3390/pathogens9030231.
- [38] Goicoechea M, Cámara L, Macías N, Muñoz A, de Morales Á, Rojas G, et al. COVID-19: clinical course and outcomes of 36 hemodialysis patients in Spain. *Kidney Int*. 2020;98(1):27–34. doi: 10.1016/j.kint.2020.04.031.
- [39] Weigang L, Jorge Pinto Alves C, Omar N. An expert system for air traffic flow management. *J Adv Transport*. 1997;31:343–61. doi: 10.1002/atr.5670310308.
- [40] Svoboda P, Karner W, Rupp M. Traffic analysis and modeling for world of warcraft. *IEEE International Conference on Communication–2007*. Glasgow: 2007. doi: 10.1109/ICC.2007.270.
- [41] Gössling S. Risks, resilience, and pathways to sustainable aviation: A COVID-19 perspective. *J Air Transp Manag*. 2020;89:101933. doi: 10.1016/j.jairtraman.2020.101933.
- [42] Louzada-Neto F, Cancho VG, Barriga DCG. The Poisson-exponential distribution: A Bayesian approach. *J Appl Stat*. 2011;38(6):1239–48. doi: 10.1080/02664763.2010.491862.
- [43] Valjarević A, Valjarević D, Stanojević-Ristić Z, Djekić T, Živić N. A geographical information systems-based approach to health facilities and urban traffic system in Belgrade. *Serb Geospat Health*. 2018;13:308–13. doi: 10.4081/gh.2018.729.
- [44] Valjarević A, Srećković-Batočanin D, Valjarević D, Matović V. A GIS-based method for analysis of a better utilization of thermal-mineral springs in the municipality of Kursumlija (Serbia). *Renewable Sustainable Energy Rev*. 2018;92:948–57.
- [45] Sullivan GM, Artino AR Jr. Analyzing and interpreting data from likert-type scales. *J Graduate Med Educ*. 2013;5:541–2.
- [46] Wright JK. Crossbreeding geographical quantiles. *Geograph Rev*. 1955;45:52–65.
- [47] Robinson AH, Morrison JL, Muehrcke PC, Kimerling JA, Guptill SC. *Elements of Cartography* 1995. 6th edn. Canada, Ottawa: John Wiley and Sons; 1995.
- [48] Wang H, Wang Z, Dong Y, Chang R, Xu C, Yu X, et al. Phase-adjusted estimation of the number of Coronavirus Disease 2019 cases in Wuhan, China. *Cell Discovery*. 2020;6:10. doi: 10.1038/s41421-020-0148-0.
- [49] Liu Y, Gayle AA, Wilder-Smith A, Rocklöv J. The reproductive number of COVID-19 is higher compared to SARS coronavirus. *J Travel Med*. 2020;27:1. doi: 10.1093/jtm/taaa021.
- [50] Xu Z, Shi L, Wang Y, Zhang J, Huang L, Zhang C, et al. Pathological findings of COVID-19 associated with acute respiratory distress syndrome. *Lancet Respir Med*. 2020;8:420–22. doi: 10.1016/S2213-2600(20)30076-X.
- [51] Andersen L, Harden S, Sugg M, Runkle J, Lundquist T. Analyzing the spatial determinants of local covid-19 transmission in the United States. *Sci Total Env*. 2020;754:142396. doi: 10.1016/j.scitotenv.2020.142396.
- [52] Sun F, Matthews SA, Yang T, Hu M. A spatial analysis of the COVID-19 period prevalence in U.S. counties through June 28, 2020: Where geography matters? *Ann Epidemiol*. 2020. doi: 10.1016/j.annepidem.2020.07.014.
- [53] Hadjidemetriou GM, Sasidharan M, Kouyialis G, Parlikad AK. The impact of government measures and human mobility trend on COVID-19 related deaths in the UK. *Trans Res Interdiscip Perspect*. 2020;6:100167. doi: 10.1016/j.trip.2020.100167.
- [54] Tiirinki H, Tynkkynen LK, Sovala M, Atkins S, Koivusalo M, Rautiainen P, et al. COVID-19 pandemic in Finland—Preliminary analysis on health system response and economic consequences. *Health Policy Technol*. 2020;9(4):642–62. doi: 10.1016/j.hlpt.2020.08.005.
- [55] Jin L, Zhao Y, Zhou J, Tao M, Yang Y, Wang X, et al. Distributions of time, place, and population of novel coronavirus disease 2019 (COVID-19) from January 20 to February 10, 2020, in China. *Rev Clín Española*. 2020;220(8):495–500. doi: 10.1016/j.rce.2020.04.001.
- [56] Sun F, Matthews SA, Yang T, Hu M. A spatial analysis of the COVID-19 period prevalence in U.S. counties through June 28, 2020: Where geography matters? *Ann Epidemiol*. 2020; Jul. doi: 10.1016/j.annepidem.2020.07.014.
- [57] Pai C, Bhaskar A, Rawoot V. Investigating the dynamics of COVID-19 pandemic in India under lockdown. *Chaos Solitons Fractals*. 2020;138:109988. doi: 10.1016/j.chaos.2020.109988.
- [58] Gharakhanlou NM, Hooshangi N. Spatio-temporal simulation of the novel coronavirus (COVID-19) outbreak using the agent-based modeling approach (case study: Urmia, Iran). *Inform Med Unlocked*. 2020;20:100403. doi: 10.1016/j.imu.2020.100403.
- [59] Mbunge E. Effects of COVID-19 in South African health system and society: An explanatory study. *Diabetes Metab Syndrome Clin Res Rev*. 2020;14:1809–14. doi: 10.1016/j.dsx.2020.09.016.